JOURNAL OF GEOPHYSICAL RESEARCH, VOL. 104, NO. B9, PAGES 20,449-20,466, SEPTEMBER 10, 1999

Sequence stratigraphy, structure, and tectonic history of the southwestern Ontong Java Plateau adjacent to the North Solomon Trench and Solomon Islands arc

Eric J. Phinney[1]
Department of Geological Sciences and Institute for Geophysics, University of Texas at Austin

Paul Mann, Millard F. Coffin, and Thomas H. Shipley
Institute for Geophysics, University of Texas at Austin

Abstract. The Ontong Java Plateau (OJP) is the largest and thickest oceanic plateau on Earth and one of the few oceanic plateaus actively converging on an island arc. We present velocity determinations and geologic interpretation of 2000 km of two-dimensional, multi-channel seismic data from the southwestern Ontong Java Plateau, North Solomon Trench, and northern Solomon Islands. We recognize three megasequences, ranging in age from early Cretaceous to Quaternary, on the basis of distinct interval velocities and seismic stratigraphic facies. Megasequence OJ1 is early Cretaceous, upper igneous crust of the OJP and correlates with basalt outcrops dated at 122-125 Ma on the island of Malaita. The top of the overlying megasequence OJ2, a late Cretaceous mudstone unit, had been identified by previous workers as the top of igneous basement. Seismic facies and correlation to distant Deep Sea Drilling Project/Ocean Drilling Program sites indicate that OJ2 was deposited in a moderately low-energy, marine environment near a fluctuating carbonate compensation depth that resulted in multiple periods of dissolution. OJ2 thins south of the Stewart Arch onto the Solomon Islands where it is correlated with the Kwaraae Mudstone Formation. Megasequence OJ3 is late Cretaceous through Quaternary pelagic cover which caps the Ontong Java Plateau; it thickens into the North Solomon Trench, and seismic facies suggest that OJ3 was deposited in a low-energy marine environment. We use seismic facies analysis, sediment thickness, structural observations, and quantitative plate reconstructions of the position of the OJP and Solomon Islands to propose a tectonic, magmatic, and sedimentary history of the southwestern Ontong Java Plateau. Prior to 125 Ma late Jurassic and early Cretaceous oceanic crust formed. From 125 to 122 Ma, the first mantle plume formed igneous crust (OJ1). Between 122 and 92 Ma, marine mudstone (OJ2 and Kwaraae mudstone of Malaita, Solomon Islands) was deposited on Ontong Java Plateau. At 92 Ma a second mantle plume caused widespread volcanism on the plateau. From 92 to 15 Ma, pelagic carbonate sediment (OJ3) was deposited. At ~15 Ma the southern Ontong Java Plateau was deformed by normal faults during its approach toward the North Solomon Trench. Finally, from 4 to 0 Ma, the Malaita Accretionary Prism formed during collision between a substantially thicker portion of the Ontong Java Plateau and the Solomon Islands arc. Flexure of the Ontong Java Plateau near the trench caused coeval normal faulting.

1. Introduction

The Ontong Java Plateau (OJP), located in the west central Pacific Ocean, is the world's largest oceanic plateau (Figure 1). This large igneous province covers ~1.86 x 10^6 km^2 [*Coffin and Eldholm*, 1994] with an estimated total volume of 56.7 x 10^6 km^3 [*Gladczenko et al.*, 1997]. The OJP is adjacent to the Lyra, East Mariana, and Nauru Basins and is bounded to the south by the North Solomon Trench and Solomon Islands (Figure 1a). The islands of Ulawa, Malaita, and the northern part of Santa Isabel are exposed sections of the plateau resulting from mid-Pliocene accretion of the Malaita Accretionary Prism (MAP) during southwest directed subduction of the Pacific plate beneath the island arc [*Hughes and Turner*, 1977; *Petterson*, 1995; *Mann et al.*, 1996; *Neal et al.*, 1997] (Figure 1b). The extent of deformation of the southern OJP at the North Solomon Trench increases from northwest to southeast. Upper sedimentary reflections are relatively continuous on the plateau

[1]Now at BP/Amoco, Houston, Texas.

Paper number 1999JB900169.
0148-0227/99/1999JB900169$09.00

except where cut by extensional faults related to flexure of the OJP at its outer forebulge adjacent to the North Solomon Trench (Stewart Arch, Figure 1b).

Lithology, stratigraphy, geochemical analyses, and radiometric dating have been used to correlate the deformed sections of the OJP in the Solomons with Ocean Drilling Program (ODP) and Deep Sea Drilling Project (DSDP) drilling results on the main, relatively undeformed plateau [*Winterer et al.*, 1971; *Kroenke*, 1972; *Shipboard Scientific Party*, 1975a, b, 1986, 1991a, b; *Hughes and Turner*, 1976, 1977; *Berger et al.*, 1991; *Petterson*, 1995; *Tejada et al.*, 1996; *Neal et al.*, 1997; *Petterson et al.*, 1997]. The OJP has been drilled a number of times by DSDP and ODP since the late 1960s (Figure 1b). A similar stratigraphic succession has been found at most locations [*Winterer et al.*, 1971; *Shipboard Scientific Party*, 1975a, b, 1986, 1991a, b]. The stratigraphic column can generally be divided into four main units: (1) early and late Cretaceous pillow basalt, massive basalt flows, and interbedded limestone with vitric tuff sequences emplaced at 122 ± 0.9 Ma and 92 ± 1.6 Ma [*Tejada et al.*, 1996]; (2) Cretaceous claystone, siltstone, and limestone deposited in the interval between the first and second igneous pulses (122-92 Ma); (3) late Cretaceous to Eocene nannofossil chalk, limestone, and chert (92-45 Ma); and (4) middle Eocene through present nannofossil ooze and chalk (45-0 Ma). Only three drill sites have penetrated basalt from the OJP: DSDP Site 289 (9.2 m), ODP Site 803 (26 m), and ODP Site 807 (149 m). Although both igneous sequences have never been drilled at the same location on the OJP, they are present together on the island of Santa Isabel [*Tejada et al.*, 1996].

Intrabasement reflections within the basaltic crust of the OJP were first identified on the southwest slope of the Stewart Arch [*Kroenke*, 1972]. *Hagen et al.* [1993] proposed that the high-impedance layer identified as basement in the northeastern OJP was actually a basalt flow underlain by sediments and that true igneous basement corresponded to the deeper intrabasement reflections. *Shipley et al.* [1993] proposed a similar interpretation for the southern Nauru Basin, where sonobuoy refraction velocities and multichannel seismic reflection images provided evidence for an older sediment and basement sequence below late Cretaceous basalt flows.

Our first objective is to use new multichannel seismic data to assess the nature of the OJP's sedimentary section using seismic sequence analysis and detailed velocity control. These techniques help to constrain lithology above intrabasement reflections and to identify a new depth to igneous basement on the southern OJP. We also refine velocity structure in the upper igneous crust of the OJP and its cap of Cenozoic sedimentary rocks.

Our second objective is to document development of the southern OJP using structural and stratigraphic relationships. In addition to the most recent phase of faulting related to subduction, evidence for earlier deformation exists which adds insight to the Cretaceous and early Tertiary tectonic history of the OJP. A previously unidentified Cretaceous sedimentary megasequence beneath a younger pelagic megasequence indicates a depositional environment different from the long recognized and much better studied pelagic carbonate section deposited during the Cenozoic.

Our third objective is to interpret the main igneous, tectonic, and sedimentary events affecting OJP by presenting quantitative plate reconstructions of the OJP at the critical periods of 122, 92, 45, and 13 Ma. These reconstructions suggest the importance of hot spots in localizing igneous and deformational events on OJP at 122 and 92 Ma.

2. Data Used in This Study

We acquired >2000 km of two-dimensional marine multichannel seismic data across the northern Solomon Islands and OJP aboard the R/V *Maurice Ewing* in late 1995 (Figure 1c). Line 1 from this survey (EW95-11) extends 160 km onto the OJP and provides the basis for this study. Streamer length was 3000 m with a receiver group spacing of 25 m. The 20-element, 8510 inch^3 air gun array was fired at a randomized 20 s. Nonuniform ship speed resulted in variable shot spacing and fold in the common midpoint (CMP) gathers. In an attempt to increase signal within the deeper layers of the OJP, CMP supergathers (120 maximum fold) were grouped every 50 m by binning four consecutive normal CMPs. Velocity analyses were performed approximately every 2500 m along line 1. Normal move-out correction was followed by an internal mute of the near 1000 m offsets just above the water column multiple. Next, the data were stacked and fx (frequency-distance) migrated. A band-pass filter and automatic gain control were applied to some displays (Figures 2, 3, and 6); relative amplitudes have been preserved for the remainder of seismic images shown.

3. Data Intepretation

3.1 Megasequence OJ1

We interpret OJ1 as igneous basement with the sediment/basement contact labeled as reflection R21 (Figure 2). Internal reflections within OJ1 dip to the southwest at 6° and

Figure 1. (a) Location map of study area in the southwest Pacific Ocean. (b) Outline of the Ontong Java Plateau (OJP) (light gray) defined in general by the 4000 m isobath and the Malaita Accretionary Prism (MAP, dark gray). Dashed line indicates the crest of the outer bulge related to flexure of the OJP as inferred from satellite derived free-air gravity [*Sandwell and Smith*, 1997]. Thin black lines are Mesozoic magnetic anomalies from *Nakanishi et al.* [1992] and *Cande et al.* [1989]. Plate vector was calculated from NUVEL-1A model [*DeMets et al.*, 1994] using a fixed Australian plate. Bathymetric data are from ETOP0-5 with a 1000 m contour interval. (c) Regional seismic control for the Solomon Islands-Ontong Java Plateau study area and location of subduction zones. EW95-11 multichannel seismic lines are solid, and single-channel seismic lines from *Kroenke* [1972] are dashed. The thick black line indicates the portion of line 1 shown in Figure 2; box denotes the area illustrated in Figure 4. Abbreviations are: CH, Choiseul; CJT, Cape Johnson Trench; G, Guadalcanal; KKKF, Kia-Kaipito-Korigole fault system; M, Malaita; NBT, New Britain Trench; NG, New Georgia Group; NST, North Solomon Trench; SA, Stewart Arch; SCT, San Cristobal Trench; SI, Santa Isabel; VT, Vitiaz Trench; WSR, Woodlark spreading-ridge.

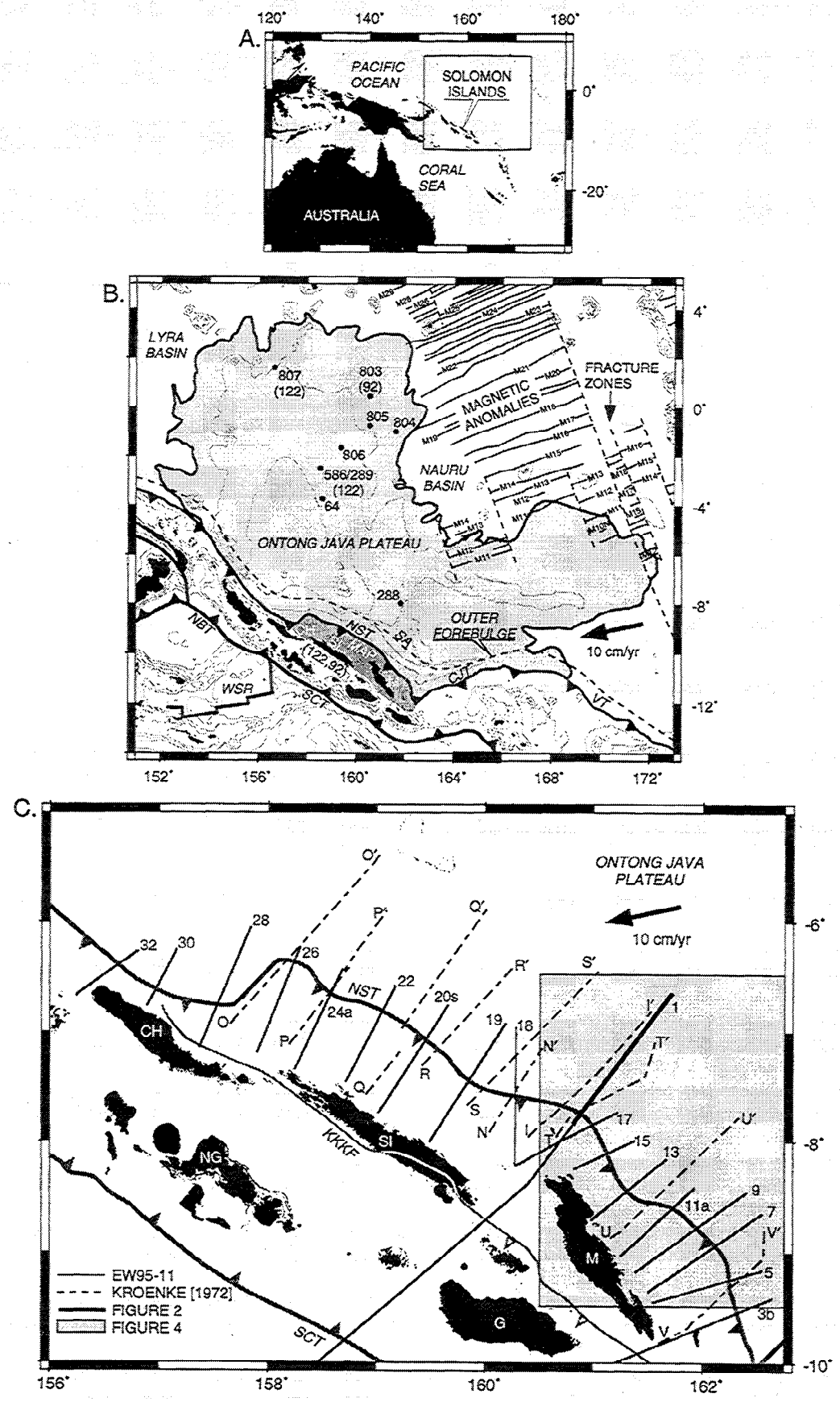
A.
120°
140°
160°
180°
PACIFIC OCEAN
SOLOMON ISLANDS
CORAL SEA
AUSTRALIA
0°
-20°
B.
LYRA BASIN
807 (122)
803 (92)
805
804
806
586/289 (122)
64
MAGNETIC ANOMALIES
FRACTURE ZONES
NAURU BASIN
ONTONG JAVA PLATEAU
288
OUTER FOREBULGE
10 cm/yr
NBT
NST
SA
CIT
VT
WSR
SCT
(122,92)
4°
0°
-4°
-8°
-12°
152°
156°
160°
164°
168°
172°
C.
ONTONG JAVA PLATEAU
10 cm/yr
CH
NG
SI
KKKF
SCT
G
M
NST
EW95-11
KROENKE [1972]
FIGURE 2
FIGURE 4
-6°
-8°
-10°
156°
158°
160°
162°

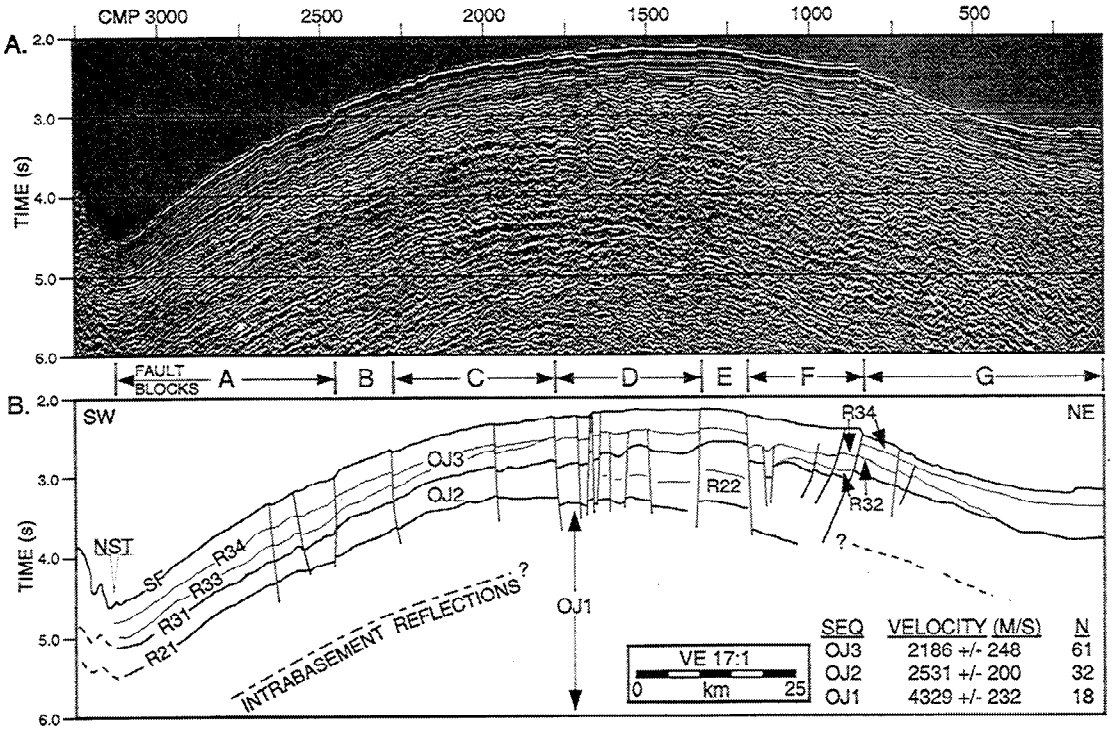

Figure 2. EW95-11 line 1 with line drawing denoting megasequences and horizons. Inset table summarizes mean interval velocity for each megasequence with *N* being the number of CMPs used. The velocity model for line 1 is a smoothed function of the interval velocities computed from reliable picks in the stacking velocity functions. A further breakdown of lateral changes in velocity within each megasequence is listed in Table 1. A-G are fault blocks delineated by faults traceable to adjacent lines I-I′ and T-T′ [*Kroenke*, 1972]. Major reflections are designated by "R" and are referred to in text. Abbreviations are: NST, North Solomon Trench; SF, seafloor.

are traceable 65 km along line 1 northeast of the North Solomon Trench. The interval between the top of basement (R21) and the deepest intrabasement reflections ranges from 1.0 to 2.5 km in thickness, with a general increase in thickness toward the North Solomon Trench. OJ1 primarily consists of low-amplitude, subparallel, semicontinuous reflections. These reflections obliquely intersect coherent background noise through fault blocks A and B. Based on differential moveout observed during velocity analysis, some intrabasement reflections may be peg-leg multiples originating from the overlying OJ2 and OJ3 megasequences or converted modes from sediment-basalt or basalt-basalt interfaces.

R21 is a high-amplitude, semicontinuous reflection (Figure 2). It can be traced from the North Solomon Trench through fault block F; it becomes less prominent farther northeast, although it is still recognizable. In fault blocks B-D, R21 is overlain by a reflection-free interval 100-300 ms thick, indicating a relatively homogeneous layer above basalt (Figure 2). Based on the 1300-1800 m/s increase in seismic interval velocity below R21 (Table 1) and the distinct change in seismic character above R21 (megasequence OJ2, following section), we correlate R21, the base of OJ2, with the top of Early Cretaceous basalt exposed in the MAP (Figure 3). Several high-amplitude, discontinuous reflections at the base of OJ2 suggest that the sediment/basalt transition consists of several thin basalt flows with interbedded sediment. These thin flows are underlain by more massive flows that are thought to make up the majority of the 32 to 35-km-thick crust of the southwestern OJP [*Coffin and Eldholm*, 1994; *Miura et al.*, 1996; *Gladczenko et al.*, 1997].

We are unable to correlate the observed intrabasalt reflections (Figure 2) below R21 with any units in the massive, deformed, shallow basaltic section exposed on Malaita [*Petterson*, 1995; *Petterson et al.*, 1997; *Neal et al.*, 1997]. We assume that the low-amplitude, intrabasement reflections within OJ1, which run parallel to the overlying OJ2 along line 1 (Figure 2), arise from a series of flows and/or sediment interbeds thicker than any such flows or beds mapped on Malaita [*Petterson*, 1995; *Petterson et al.*, 1997] (Figure 3a) or sampled at DSDP/ODP sites on the northern OJP (Figure 1b). There are no drill sites located within the MAP or near the North Solomon Trench to aid in tying the structurally complex geology in the Solomon Islands to seismic data from the OJP. At the closest drill site, DSDP Site 288, located ~77 km from the northern end of line 1 (Figure 1b), igneous basement was neither penetrated by drilling nor identified on single-channel seismic data [*Shipboard Scientific Party*, 1975a] (Figures 3d and 3e).

Velocity analyses on the intrabasement reflections for the uppermost part of OJ1 (CMP 1950-3050 on Figure 2) yielded interval velocity values of 4.3±0.2 km/s (Table 1). This multichannel seismic velocity range disagrees somewhat with 4.9 to 5.3 km/s for the upper igneous crust [*Miura et al.*, 1996].

The discrepancy between reflection and refraction velocities can be attributed to differences in raypaths of reflected and refracted waves. First arrival refracted waves travel horizontally over tens of kilometers in high-velocity basalt layers, while the much shorter ray paths of reflected waves travel greater percentages of distance vertically and are less weighted by high-velocity basalt.

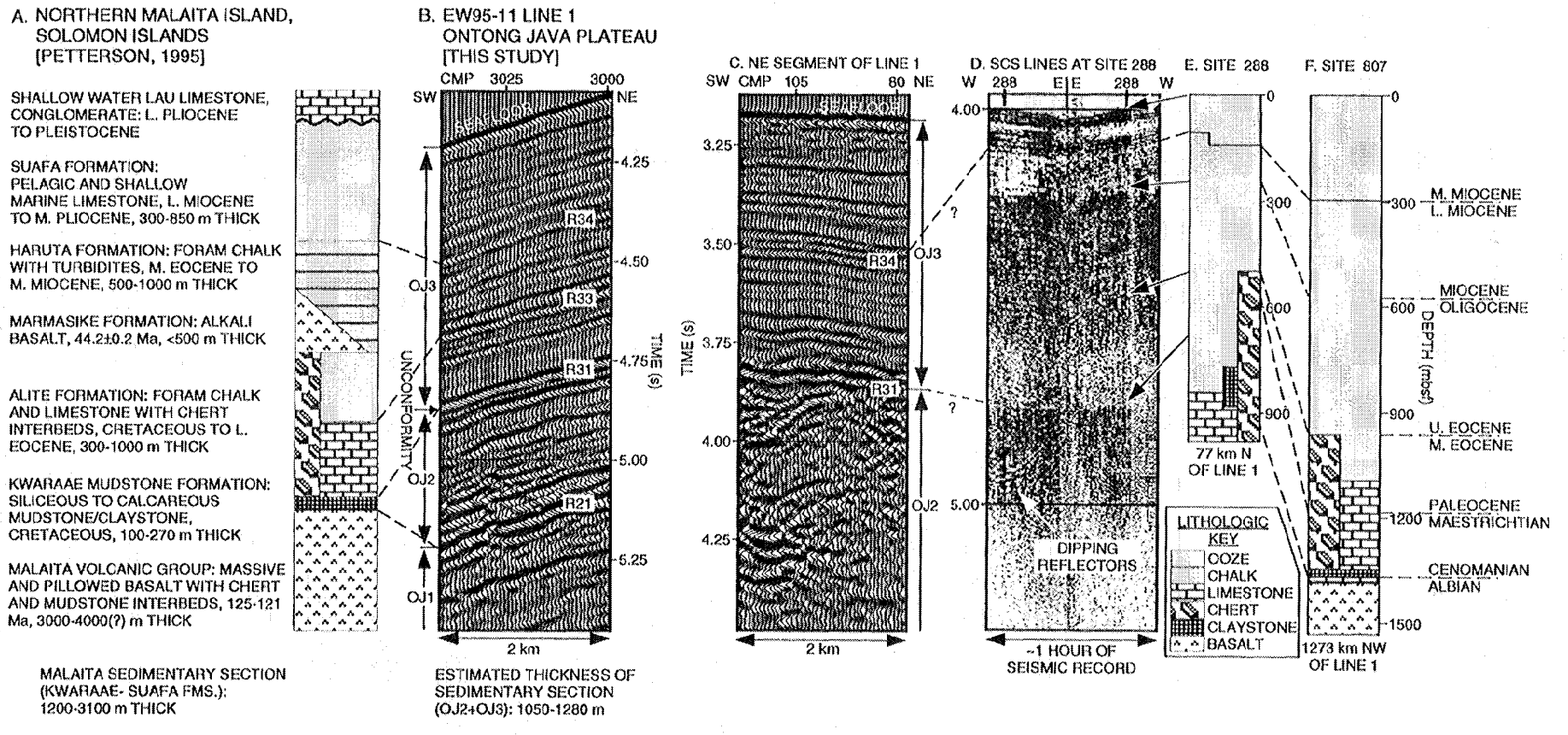

Figure 3. Correlation of line 1 with northern Malaita stratigraphy, DSDP Site 288 single-channel seismic data, and Sites 288 and 807 stratigraphy. (a) Northern Malaita stratigraphy. Stratigraphic column, lithologic descriptions, thicknesses and ages are from northern part of Malaita island [*Petterson*, 1995]. (b) Southwest segment of Line 1. (c) Northeast segment of line 1 multichannel seismic data. (d) Single-channel seismic data collected over DSDP Site 288 tied to stratigraphic column from Site 288 shown in Figure 3c. (e) Stratigraphic column from DSDP Site 288 [*Shipboard Scientific Party*, 1975a]. (f) Stratigraphic column from ODP Site 807 [*Shipboard Scientific Party*, 1991b]. Correlation of line 1 with seismic and well data is discussed in text. Inset provides key to lithologies.

Table 1. Averaged Interval Velocities Derived From Multichannel Seismic Line 1 for Megasequences OJ1, OJ2, and OJ3.

Mega Sequence	CMP Range	Velocity, m/s	s.d., m/s	*N*
OJ3	102-3202	2186	248	61
	102-402	2297	157	8
	430-1330	1999	86	18
	1402-2402	2080	92	19
	2430-3202	2347	52	16
OJ2	875-1320	3047	172	8
	1402-3102	2531	200	32
OJ1	2002-2102, 2235-2502, 2602-3033	4329	232	18

See Figure 1 for location of Line 1 and Figure 2 for location of common midpoints (CMP). *N* represents the number of CMPs used to compute the average interval velocity and standard deviation.

3.2 Megasequence OJ2

OJ2 is the deepest and oldest sedimentary megasequence on the southwestern OJP. OJ2 is bounded at its base by R21, the top of igneous basement, and at its top by a prominent, high-amplitude reflection (R31, Figure 2). OJ2 thickens northeastward from the North Solomon Trench until its basal reflection (R21) is no longer visible within block F. The megasequence can be mapped in several seismic lines within and northeast of the MAP (Figure 4). OJ2 isopachs trend obliquely to the tectonic strike of rocks on Malaita, and the megasequence generally thins to the southwest with a secondary trend thinning to the south. OJ2 pinches out along an interval of line 17 and is block-faulted by N-S striking normal faults at the northeast ends of lines 7 and 9 (Figure 4). Faults affecting OJ2 northeast of southern Malaita (lines 7 and 9) appear to mark uplift and erosion of OJ2, because the faults do not penetrate the overlying OJ3 pelagic section. OJ2 is not visible

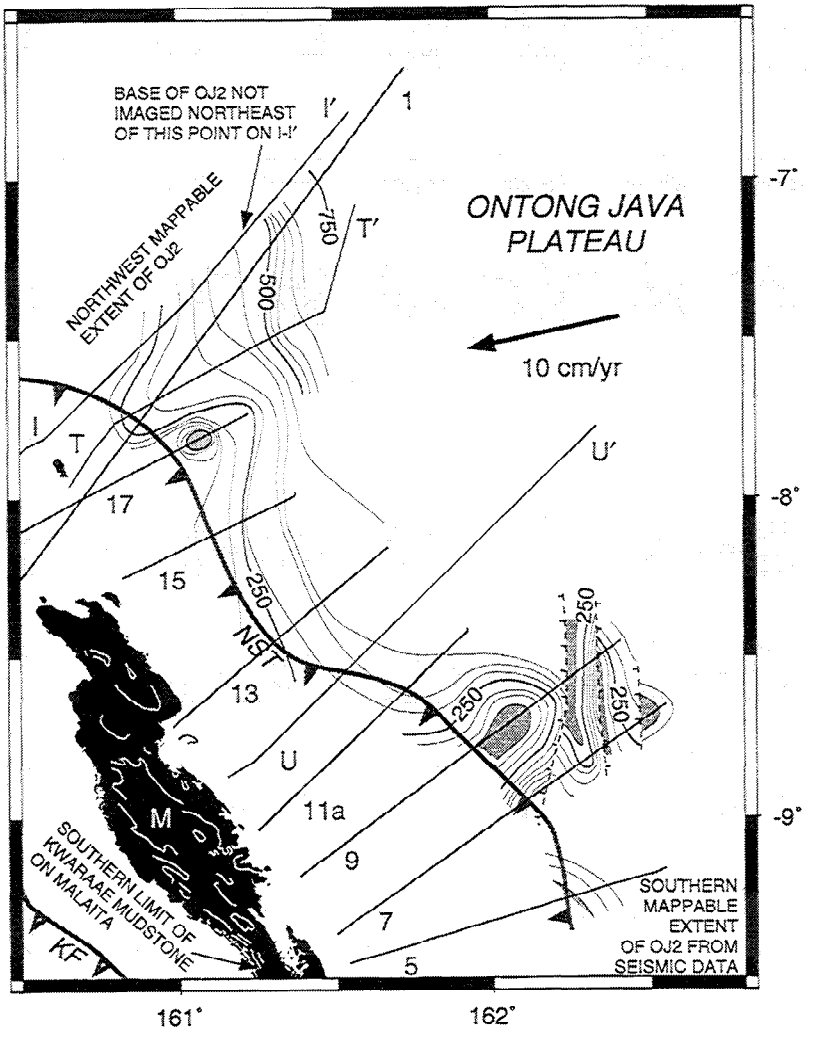

Figure 4. Isochron map of OJ2 as interpreted from multiple EW95-11 seismic lines and lines I-I′ and T-T′ [*Kroenke*, 1972]. Areas of thinnest OJ2 sediment are shaded gray. OJ2 temporal thicknesses were recorded every 50-100 m and are contoured by hand. Isopach contour interval for OJ2 is 50 ms. Data values from line U-U′ were unreliable and were not used in map construction. Dashed lines denote faults imaged in seismic data with fault strikes inferred from lineaments in satellite-derived free-air gravity anomalies [*Sandwell and Smith*, 1997]. Outcrops of the Kwaraae Mudstone Formation (KMF) in white were taken from *Petterson* [1995] and *Hughes and Turner* [1976]. Abbreviations are: KF, Kaipito Fault; M, Malaita; NST, North Solomon Trench.

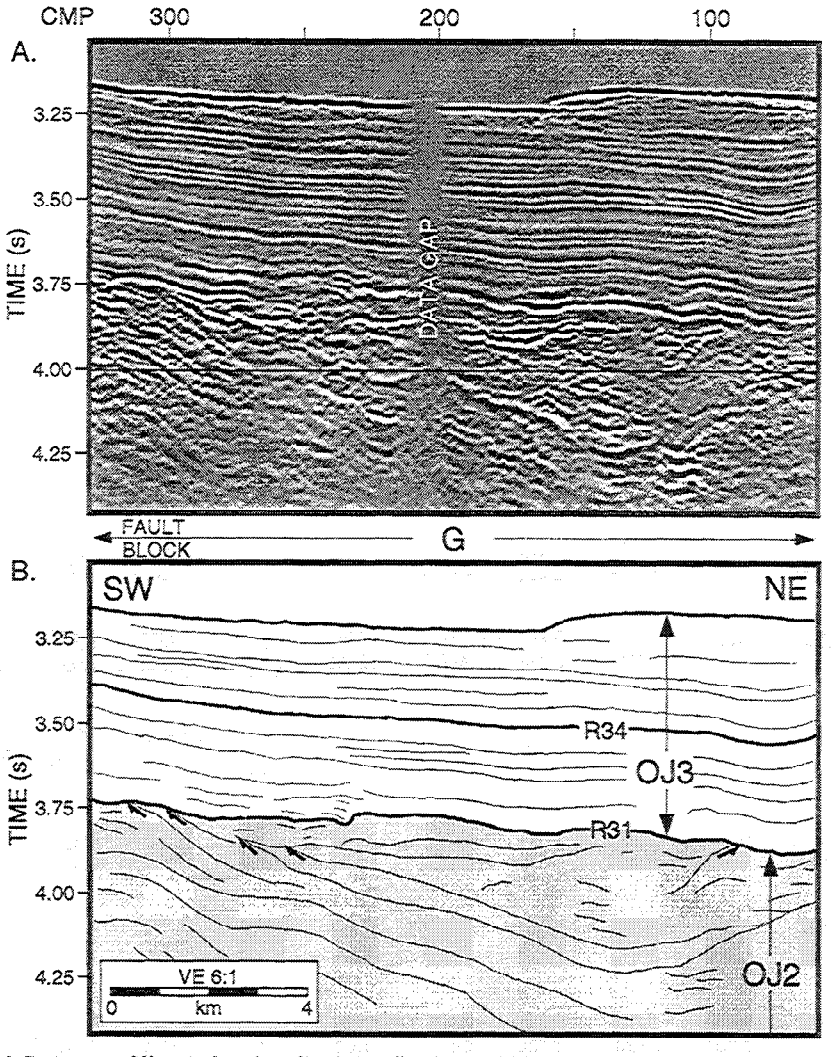

Figure 5. (a) Segment of line 1 showing dipping reflections within OJ2. (b) Interpretation of line 1. See Figure 2 for location. OJ2 is light gray for clarity. Notice that most reflections dip to the northeast except near CMP 100 where they dip to the southwest. These reflections are erosionally truncated updip by R31. A data gap occurs between CMP 200 and CMP 215.

to the southeast of line 5, west of ine I-I′ [*Kroenke*, 1972], or on line 18 of EW95-11 (Figure 1c).

The internal reflection character of OJ2 varies considerably across line 1. Between CMP 150-350 in block G, divergent reflections dip to the northeast and are truncated by R31 (Figure 5). These moderate-amplitude, discontinuous reflections do not allow good definition of the top of OJ1. In blocks D-F, internal OJ2 reflections (R22) are subparallel to an upper series of moderate-amplitude reflections truncating against R31 in block D (Figure 6). As OJ2 thins from 600 ms in block D to <300 ms in block A, internal reflections become more chaotic and discontinuous.

OJ2 has an average interval velocity of 2531±200 m/s through blocks A-D (Figure 2 and Table 1). The interval velocity increases in blocks E and F in conjunction with the northeast thickening wedge truncated by R31 in block D (Figure 6). Interval velocities for subsections of OJ2 in block E, while highly variable, generally indicate a velocity inversion between two higher-velocity layers. An interesting phase change in R21 is observable between blocks D and E (Figure 7).

Seismic derived interval velocities, phase and amplitude of reflection R31, downhole velocity data from ODP drill sites, and stratigraphic relationships on Malaita enable us to correlate OJ2 on the southwest end of line 1 with the late Cretaceous Kwaraae Mudstone Formation on the island of Malaita (Figure 3a). As OJ2 thickens to the northeast, this correlation breaks down. We tenuously correlate OJ2 at the northeast end of line 1 with Cretaceous mudstone recovered at DSDP Site 288. Dipping reflections on the Site 288 seismic section at 4.9 s may correlate with those seen on line 1 at 4.0 s or 4.2 s (Figures 3c-3e). OJ2 reflections are discontinuous on the northeast end of line 1 making it difficult to pick velocities for a consistent horizon. However, the majority of interval velocities (2500-3400 m/s) for OJ2 in this area indicate a predominately sedimentary section.

Isopach trends are consistent with the areal extent and thinning of the Kwaraae Mudstone Formation toward southeastern Malaita (Figure 4). OJ2 thickens onto paleostructural highs of OJP but may occur throughout the plateau as a thin, detectable, but seismically unresolvable layer. A similar layer only a few meters thick was drilled at ODP Site 807 over 1000 km northwest from the northeast end of line 1 [*Shipboard Scientific Party*, 1991b] (Figure 3f). OJ2 is ~400 m thick near the North Solomon Trench, including an upper 200 m thick sec-

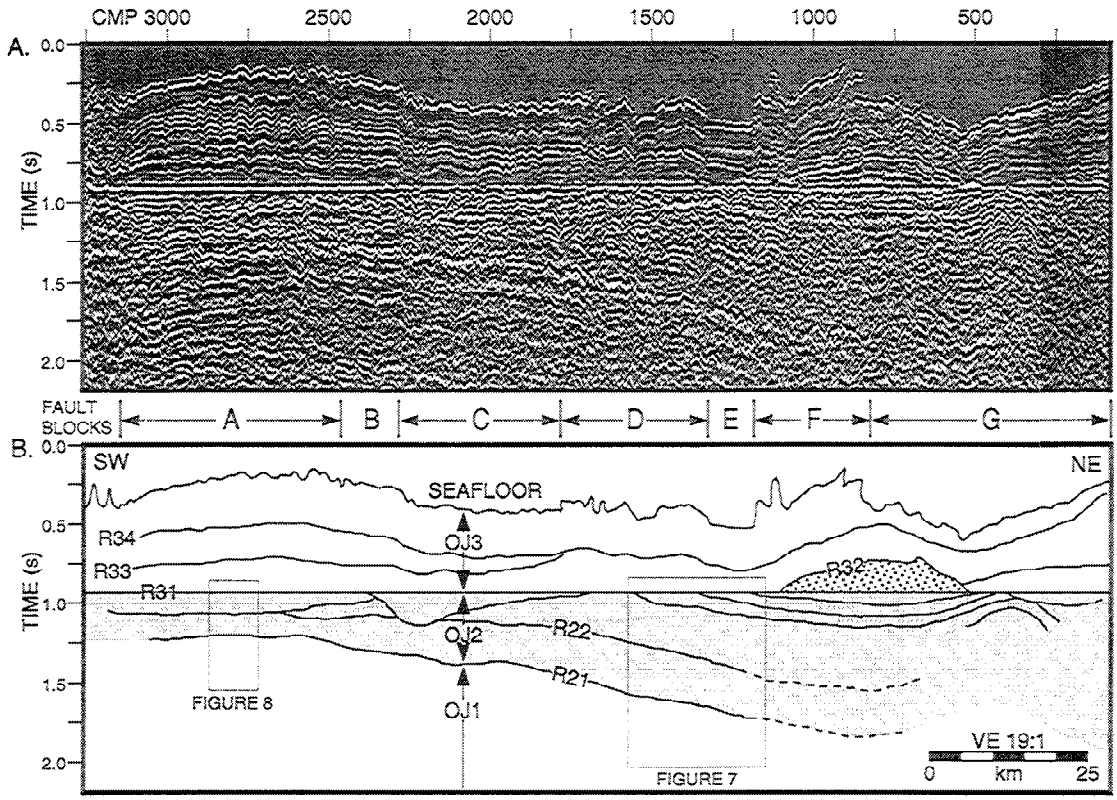

Figure 6. (a) Line 1 flattened on horizon R31. (b) Interpretation of flattened line 1. This display emphasizes significant erosion of OJ2 (gray). Boxes refer to close-ups in Figures 7 and 8. Stippled area denotes a low-velocity interval in OJ3 which may contain reworked erosional detritus from OJ2. Figure 12 shows this area flattened on horizon R32. Refer to Figure 2 for unflattened seismic section.

tion that diverges from the remainder of the unit near the trench axis at CMP 3060 (Figure 2). These values agree within a factor of two with thickness estimates for the Kwaraae Mudstone Formation on Malaita [*Petterson*, 1995; *Petterson et al.*, 1997] (Figure 3a).

R31, which marks the top of OJ2, is a high-amplitude, simple impulse response with opposite polarity to that of the similar amplitude seafloor (Figure 3b). The large amplitude and 180° phase shift of R31 is caused by a lower velocity and density in the upper OJ2 than in the overlying limestone in OJ3. Similar transitions from limestone to claystone at ODP Sites 803 and 807 show a decrease in velocity of 1000-1500 m/s and a decrease in density of 0.5 g/cm^3 [*Shipboard Scientific Party*, 1991a, b].

We propose that R31 is a subregional, late Cretaceous unconformity for three reasons: (1) correlations of R31 to a Late Cretaceous hiatus described at ODP Sites 803 and 807 [*Shipboard Scientific Party*, 1991a, b]; (2) continuity of R31 across line 1; and (3) termination of OJ2 reflections at the R31 horizon. Flattening along horizon R31 shows considerable erosion and gentle folding of OJ2 over a distance of 140 km along line 1 (Figure 6). R31 is a correlative unconformity near the North Solomon Trench and becomes an angular unconformity to the northeast. The conformable nature of R31 near the trench is in agreement with stratal geometries observed on Malaita between the Kwaraae Mudstone Formation and the overlying Alite Limestone Formation [*Petterson*, 1995]. Flattening R31 in blocks D-F emphasizes the northeast-dipping wedge of sediment in OJ2. Within block A, flattening R31 documents an acoustically transparent wedge thinning to the southwest onto the top of basalt (R21) (Figure 8). Several reflections onlap this wedge to the northeast, some of which are erosionally truncated by channels. Complex stratigraphic relationships observed in OJ2 suggest a more moderate-energy depositional environment than that of the overlying pelagic drape (OJ3).

Lateral variations in amplitude along R31 and velocity structure to the northeast of block B show that OJ2 is most likely not entirely composed of mudstone. As discussed earlier, blocks E and F are characterized by a low-velocity layer between two higher velocity layers (Figures 6 and 7). The higher-velocity layers could represent rocks with a greater percentage of carbonate content versus a lower velocity, siliceous mudstone. This sequence implies deposition near a fluctuating CCD [*Schlanger and Douglas*, 1974]; however, a more complex, vertical tectonic history cannot be ruled out. The former case is supported by semicontinuous reflections and multiple unconformities within OJ2 (Figure 8) which suggest deposition in a moderately low-energy environment near a fluctuating CCD, the latter manifested by several dissolution events. Scouring, possibly related to bottom currents, is also apparent near the top of OJ2. *Petterson* [1995] suggested that the section of Kwaraae Mudstone Formation exposed on Malaita may have passed through the CCD during deposition, based on an increase in carbonate content toward the top of the formation.

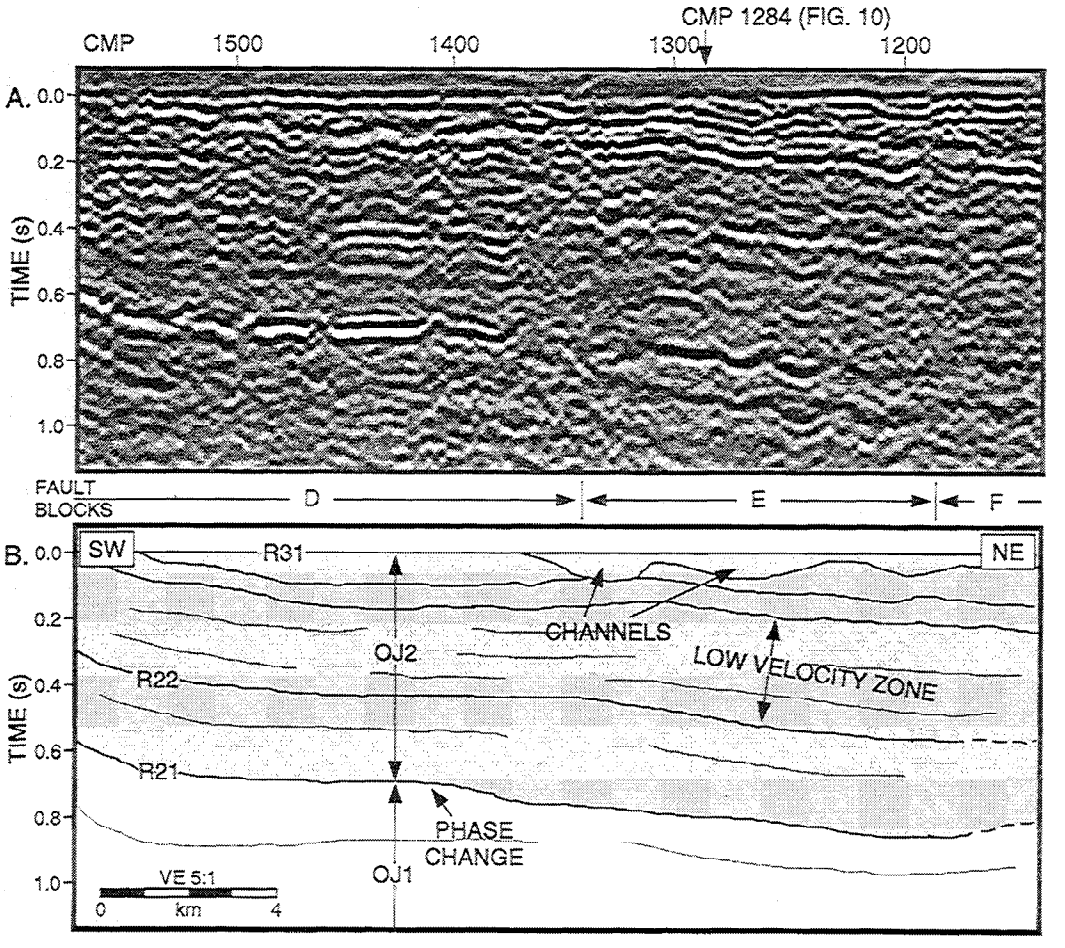

Figure 7. (a) Close-up of line 1 flattened on horizon R31 (see Figure 6 for location). (b) Interpretation of line 1. Note erosional truncation of OJ2 by R31. The low-velocity zone above R22, phase change of R21 near CMP 1350, and varying amplitude of R31 all indicate lateral changes in OJ2 lithology from the southwest where it is primarily claystone.

3.3 Megasequence OJ3

OJ3, which consists of late Cretaceous through Quaternary pelagic carbonate, varies laterally in thickness as well as velocity and reflection character (Figure 2). R31, the late Cretaceous unconformity described above, is OJ3's lower boundary, and the seafloor is its upper boundary. Laterally continuous and conformable seismic reflections within OJ3 suggest that it consists of pelagic drape deposited within a low-energy, submarine environment.

OJ3 exhibits multiple stages of Neogene to Recent faulting related to flexure of the Stewart Arch at the North Solomon Trench (Figure 9). Visual correlation of fault blocks A-G with lines I-I' and T-T' [*Kroenke*, 1972] shows an apparent westward trend oblique to the Stewart Arch (Figures 1b and 1c). The thicker OJ3 unit of block F is characterized by Miocene extensional faulting, including growth faulting during deposition of pre-R34 sediments (CMP 910 on Figure 9). The transition from block F to G is marked by 180 ms of offset, with block F downthrown. The seafloor reflection becomes rough and dips steeply to the northeast relative to the adjacent blocks (Figure 2). The rough seafloor reflection and relatively thin sediments above R34 upslope indicate a recent debris flow or slumping of the upper OJ3 section, perhaps related to normal fault scarps breaking the seafloor. An increase of 100 ms in post-R34 sediment thickness between blocks E and F (Figure 2) may also indicate some strike-slip motion.

Both above and below the prominent R34 horizon within OJ3, reflections in blocks A and B diverge slightly to the southwest as OJ3 thickens into the North Solomon Trench (Figure 2). As OJ3 thins to the northeast in block C, several reflections onlap R33 (Figure 10). The interval between R34 and R33 continues to thin to 50 ms to the northeast, where the horizons become parallel. OJ3 is thinnest (~450 ms) in block E. The interval above R34 thickens to northeast into block F, where thickness increases abruptly by 150 ms. Syndepositional ocean current scouring is apparent on the northeastern edge of block F just above horizon R34 (Figure 9).

An isopach map for OJ3 shows a range in temporal thickness of over 700 ms (Figure 11). Southwest of the Stewart Arch, OJ3 generally thickens with increasing water depth into the North Solomon Trench. Within the MAP, thicker sections of OJ3 occur on the crests of anticlines and the thinner sections on anticlinal limbs and synclines. Postdeformational terrigenous

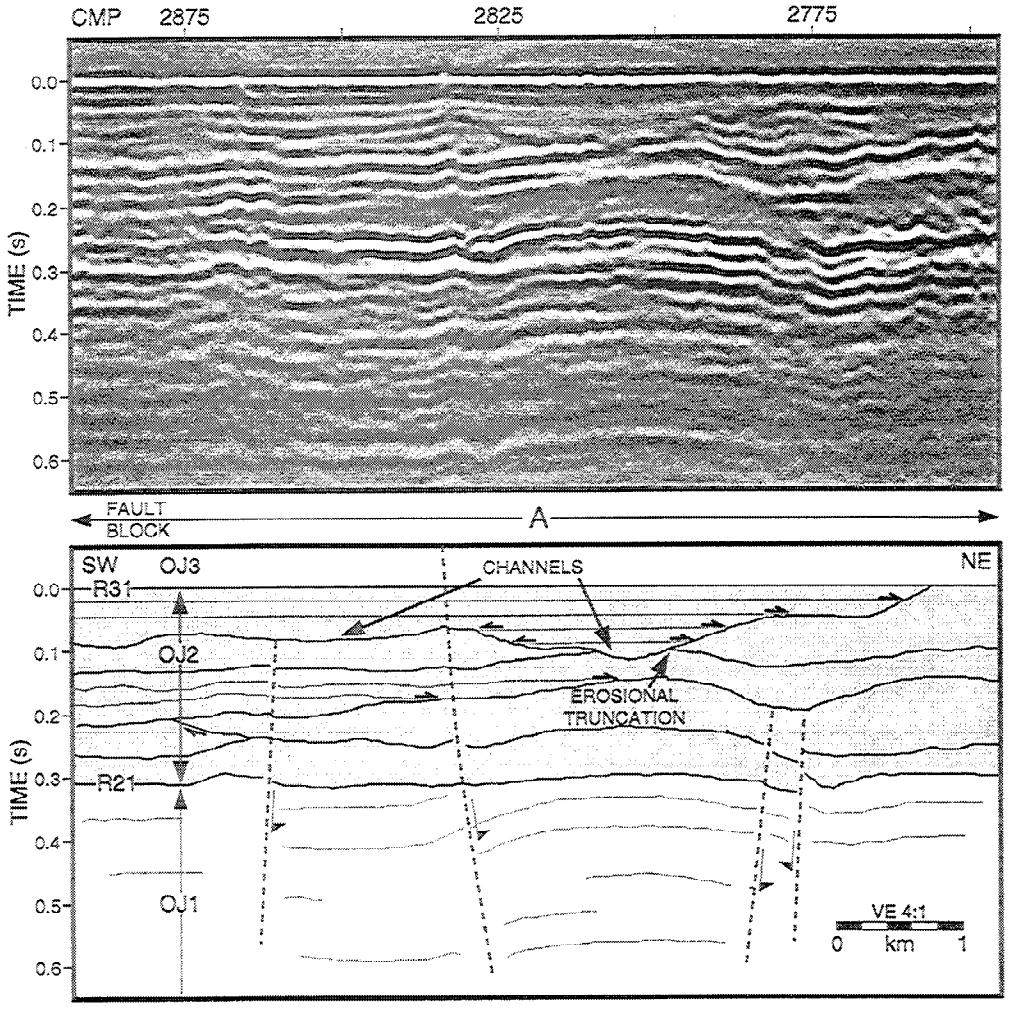

Figure 8. (a) Line drawing of line 1 flattened on R31. (b) Interpretation of line 1. See Figure 6 for location. Multiple stratigraphic patterns within OJ2 contrast with the conformable pelagic drape in OJ3. Faults denoted by dashed lines indicate several periods of faulting.

deposition and submarine slumps into the North Solomon Trench have been excluded from the isopach map.

The average interval velocity for OJ3 is 2186±248 m/s (Table 1). In block A, interval velocity for OJ3 is greatest at 2350 m/s (Figure 2). As OJ3 thins toward the Stewart Arch in blocks B-D, the velocity is lower at 2080 m/s. Velocity reaches its lowest value of 2000 m/s across the crest of the arch (blocks E-F), before increasing down the northeast dipping flank in block G. In blocks F and G, OJ3 interval velocity is weighted by a low-velocity section between horizons R31 and R32 (Figure 6). Flattening on horizon R32 shows that R31 delineates a former basin in blocks F and G based on reflections parallel to R32 and onlap against R31 (Figure 12). Interval velocity within this basin is slower than the overlying OJ3 section as shown by the decrease of 80-200 m/s in average interval velocity for OJ3 (Table 1). Low-velocity basin fill is also indicated by a 180° phase shift of the R32 reflector relative to the seafloor reflection implying a negative impedance contrast (Figure 6).

We propose that the R34 reflection correlates with the middle Miocene ooze/chalk transition between the Suafa Formation and the underlying Haruta Formation on Malaita (Figures 3a and b). Several high-amplitude reflections (labeled R33 on Figure 3b) are believed to represent the middle Eocene transition from limestone with chert interbeds to chalk with chert interbeds. Justification for tying these high-amplitude reflections to the middle Eocene chert horizon comes from core measurements at Site 807 [*Shipboard Scientific Party*, 1991b], which show significant impedance contrasts associated with the middle Eocene chert interbeds relative to the remainder of the stratigraphy (Figure 3f).

The upward progression from limestone with chert interbeds to chalk to ooze in cored sections from OJP is remarkably similar to that mapped on Malaita [*Hughes and Turner*, 1976; *Petterson*, 1995]. Although not correlative with a discrete reflection on single-channel seismic data (Figure 3d), R34 at 3.50 s (Figure 3c) may represent the ooze/chalk transition. R34 is traceable across most of line 1, and velocity spectra show an increase in stacking velocity gradient below this reflection. Increased velocity in chalk has been related to rapid decrease in porosity with depth in overlying ooze and the development of interstitial carbonate cement [*Schlanger and Douglas*, 1974]. The ooze/chalk transition is middle to late Miocene, with its depth below seafloor being inversely proportional to water depth [*Shipboard Scientific Party*, 1991b], as illustrated by comparing the stratigraphic columns of DSDP Site 288 (3030 m

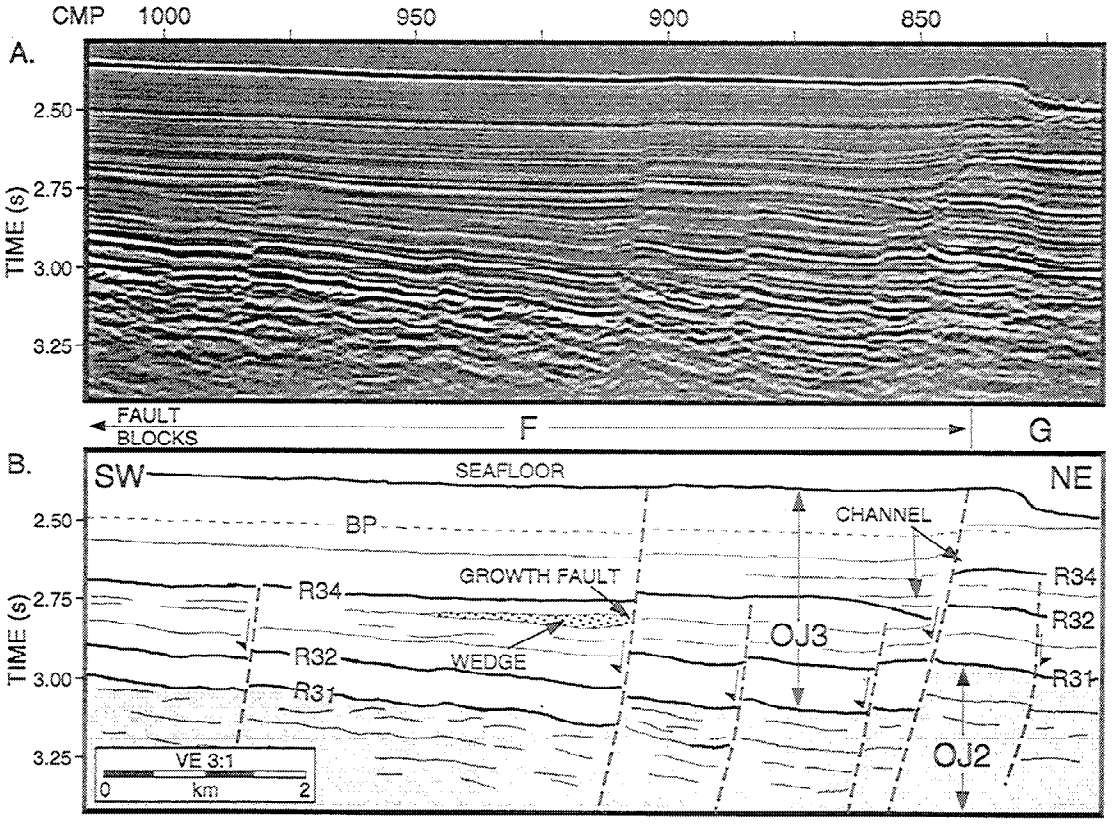

Figure 9. (a) Segment of line 1 showing evidence for multiple episodes of faulting on the southern OJP. (b) Interpretation of line 1. Faults are denoted by dashed lines. Several faults appear to terminate near R34, which is of approximately middle Miocene age. Northeast thickening of the interval between R32 and R34 near CMP 925 indicates syndepositional faulting (stippled area). This fault was reactivated during flexure of the OJP as it entered the North Solomon Trench. Erosion by paleocurrents is also observable near CMP 850 at 2.750 s.

water depth) and ODP Site 807 (2806 m water depth) (Figures 3e and 3f). The ooze/chalk and chalk/limestone transitions occur much deeper in the section at Site 807, indicating deposition at a greater distance above the CCD relative to Site 288 [*Schlanger and Douglas*, 1974; *Berger and Mayer*, 1978]. This thickness/depth relationship also holds for the northeast end of line 1 (Figure 3c) and at Site 288 (Figure 3d).

Cenozoic pelagic sediment from all OJP drill sites also show an inverse relationship between thickness and water depth. In contrast, OJ3 on the southwestern OJP thickens with increasing water depth into the North Solomon Trench (Figure 2). OJ3 equivalents on Malaita range from 970 to 2850 m thick [*Petterson*, 1995]. Using OJ3's interval velocity (Table 1), we estimate OJ3 thickness at the North Solomon Trench to be 800-900 m. This is close to the low end of *Petterson's* [1995] estimates; however, the isopach map clearly shows that OJ3 continues to thicken southwestward into the MAP (Figure 11). Also, formation thickness varies considerably on Malaita, and much of this variation may be attributed to convergent and strike-slip deformation accompanying transfer of the rocks from the obliquely converging OJP to the MAP and the Solomon Islands arc.

4. Discussion

A schematic model for OJP's tectonic evolution, based on previous studies and new observations presented herein, highlights the effects of multiple mantle plume events, deposition of the sedimentary megasequences, and deformation of the OJP during collision with the Solomon Island arc. In sections 4.1-4.6 we summarize the main events in the magmatic, tectonic, and sedimentary history of OJP highlighting contributions from the new data and our interpretation (Figure 13). We relate magmatism and tectonism affecting OJP to a regional tectonic framework using plate reconstructions at 122, 92, 45, and 13 Ma ( ). Positions of various hot spots [*Duncan and Richards*, 1991] through time, which remain fixed in a mantle framework and relative to each another, are determined by using a relative plate motion model [*Malahoff et al.*, 1982; *Auzende et al.*, 1988; *Royer et al.*, 1988; *Royer and Chang*, 1991; *Yan and Kroenke*, 1993; *Cande et al.*, 1995]. Positions of island arcs through time are derived from the ages of collision of the arc with an oceanic plateau or continental block.

4.1 Pre-125 Ma: Formation of Late Jurassic/ Early Cretaceous Oceanic Crust Later Intruded by Plume Events

No new observations bear on the existence of oceanic crust beneath OJ1 (Figure 13). Identification of magnetic anomalies [*Nakanishi et al.*, 1992; *Winterer and Nakanishi*, 1995; *Nakanishi and Winterer*, 1996] indicates large areas of Jurassic and Cretaceous crust adjacent to OJP (Figure 14a). Northwest trending fracture zones, identified from free-air gravity

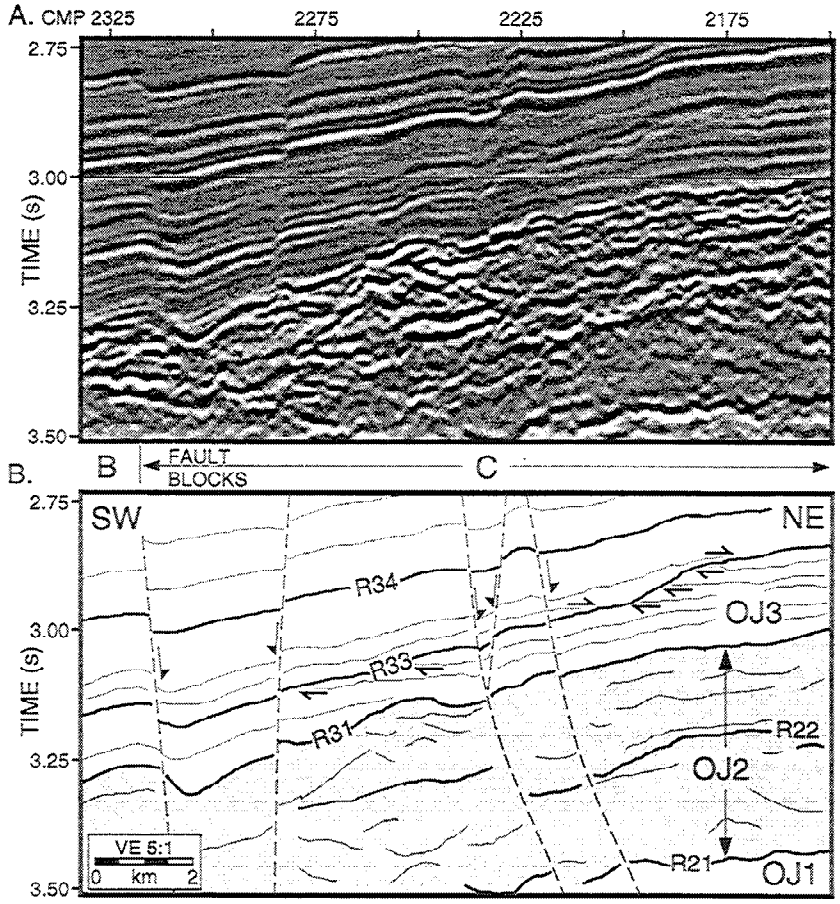

Figure 10. (a) Segment of line 1 showing reflections onlapping R33. (b) Interpretation of line 1. See Figure 2 for location. Faults are denoted by dashed lines.

lineations [*Coffin and Gahagan*, 1995; *Winterer and Nakanishi*, 1995; *Gladczenko et al.*, 1997], within this deeply buried, old oceanic crust may have been reactivated as normal faults in the outer bulge of the North Solomon Trench (Stewart Arch) (Figure 1b). Reactivation of deeply buried, older faults may explain why young faults crosscut the trend of the Stewart Arch and its southwestern bathymetric slope.

4.2 Period from 125 to 122 Ma: Formation of OJP Igneous Crust by Initial Mantle Plume, Possibly in a Near-Ridge Setting

Mantle-derived basalts, with radiometric ages from 125 to 122 Ma in the Solomon Islands (Malaita, Santa Isabel) and at ODP Sites 289, 803, and 807, constrain widespread mantle plume volcanism both on OJP and within accreted rocks of the southwestern OJP, now preserved and subaerially exposed within the MAP [*Tejada et al.*, 1995; *Neal et al.*, 1997] (Figure 1a). The Pacific plate was moving almost due west relative to the Louisville hot spot from 125 to 122 Ma (Figure 14a). The hot spot may have occupied a more central part of the OJP because an unknown amount of the western and southern edges of the OJP have been subducted or accreted at the North Solomon Trench [*Mann et al.*, 1996].

Most workers favor the idea that the initial plume event was localized and perhaps terminated by its proximity to a spreading ridge [e.g., *Winterer and Nakanishi*, 1995; *Larson*, 1997] (Figure 13). The Louisville hot spot was located beneath the southwest OJP at 122 Ma. We make no attempt to show active spreading ridges as the new data do not help to constrain the plate setting during this time; although, these data do redefine the top of acoustic basement for the southern OJP.

The remarkably smooth top of OJ2, originally interpreted as acoustic basement on single-channel seismic data [*Kroenke*, 1972, 1989], is an erosional boundary separating early to late Cretaceous mudstone of OJ2 from overlying late Cretaceous to Recent pelagic limestone of OJ3. The hypothesis of a deeper sedimentary layer and igneous basement using seismic data from the northern OJP [*Hagen et al.*, 1993] is confirmed by our data from the southern OJP. As in the southern Nauru Basin [*Shipley et al.*, 1993], better multichannel seismic data and attenuation of noise through stacking have provided more detailed images of deeper sediment.

4.3. Period from 122 to 92 Ma: Deposition of Marine Mudstone (OJ2 and Kwaraae Mudstone of Malaita, Solomon Islands) and the Second Mantle Plume Event

Multichannel seismic interval velocities and seismic stratigraphic analysis revealed a sedimentary megasequence below the pelagic cap of the plateau and above igneous basement (Figure 13). This newly recognized, intermediate unit is OJ2,

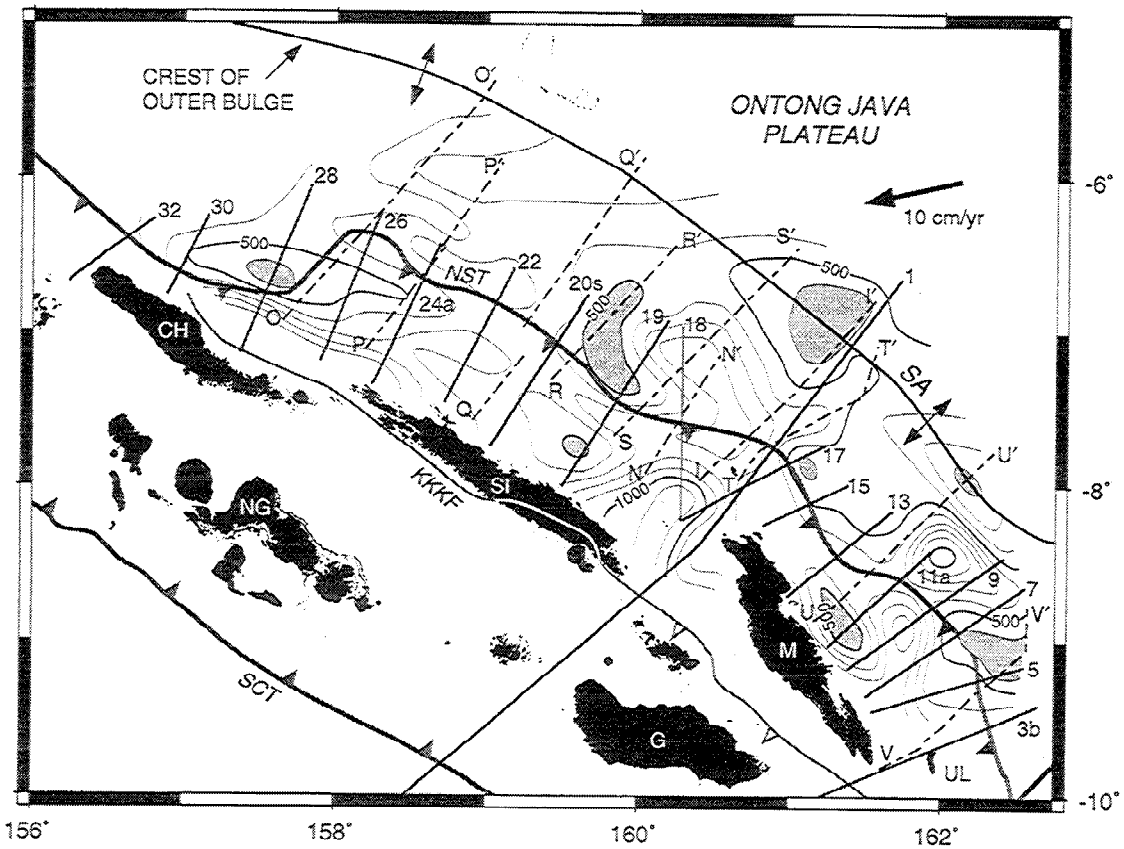

Figure 11. Isochron map of OJ3 as interpreted from 18 EW95-11 multichannel seismic lines (solid) and 10 single-channel seismic lines [Kroenke, 1972] (dashed). Areas of thinnest OJ3 sediment are shaded gray. OJ3 temporal thicknesses along solid lines were smoothed using a 25 km operator prior to contouring. Thicknesses along single-channel seismic lines were picked every 5 km northeast of the North Solomon Trench (NST) on the OJP. Contour interval is 100 ms. Abbreviations are: CH, Choiseul; G, Guadalcanal; KKKF, Kia-Korigole-Kaipito fault system; M, Malaita; NG, New Georgia Group; SA, Stewart Arch; SCT, San Cristobal Trench; SI, Santa Isabel; UL, Ulawa.

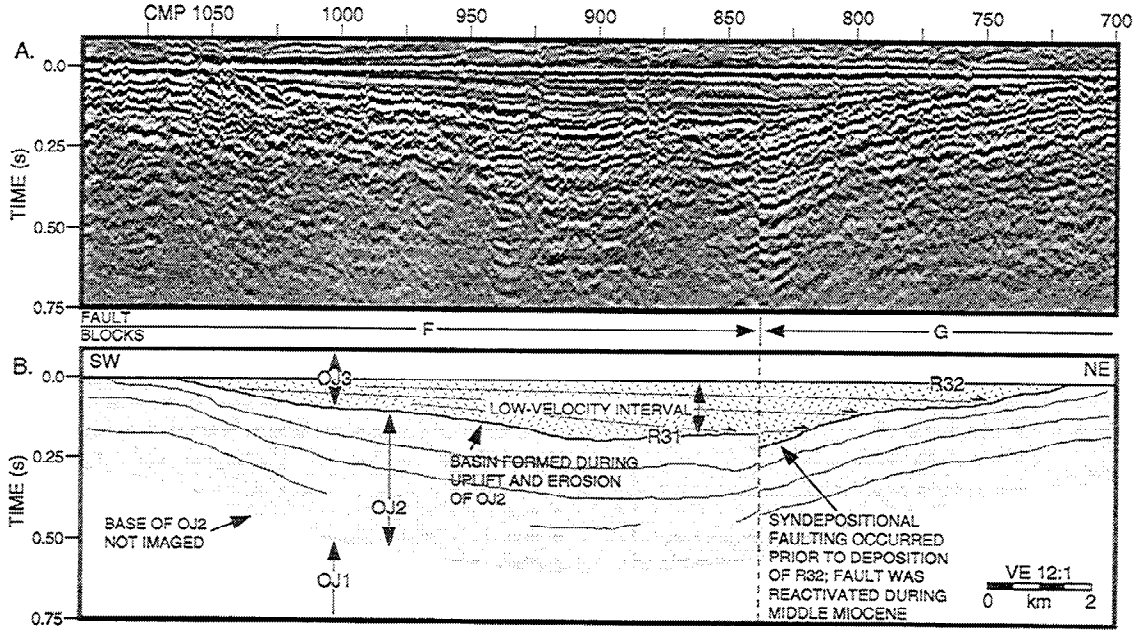

Figure 12. (a) Line 1 flattened on the R32 horizon. (b) Interpretation of line 1. See Figure 6 for location. Onlapping relationships between R32 and R31 imply that this section of plateau was gently folded and became a depocenter for eroded OJ2 detritus (stippled region). Folding occurred prior to the Lower Cenomanian, possibly related to the 92 Ma mantle plume event.

which we infer to be of Barremian-Albian age based on radiometric dating of Malaita basalts at 122 Ma [*Tejada et al.*, 1995] and pre-Cenomanian paleontologic age of a correlative unit, the Kwaraae Mudstone Formation of Malaita [*Petterson*, 1995].

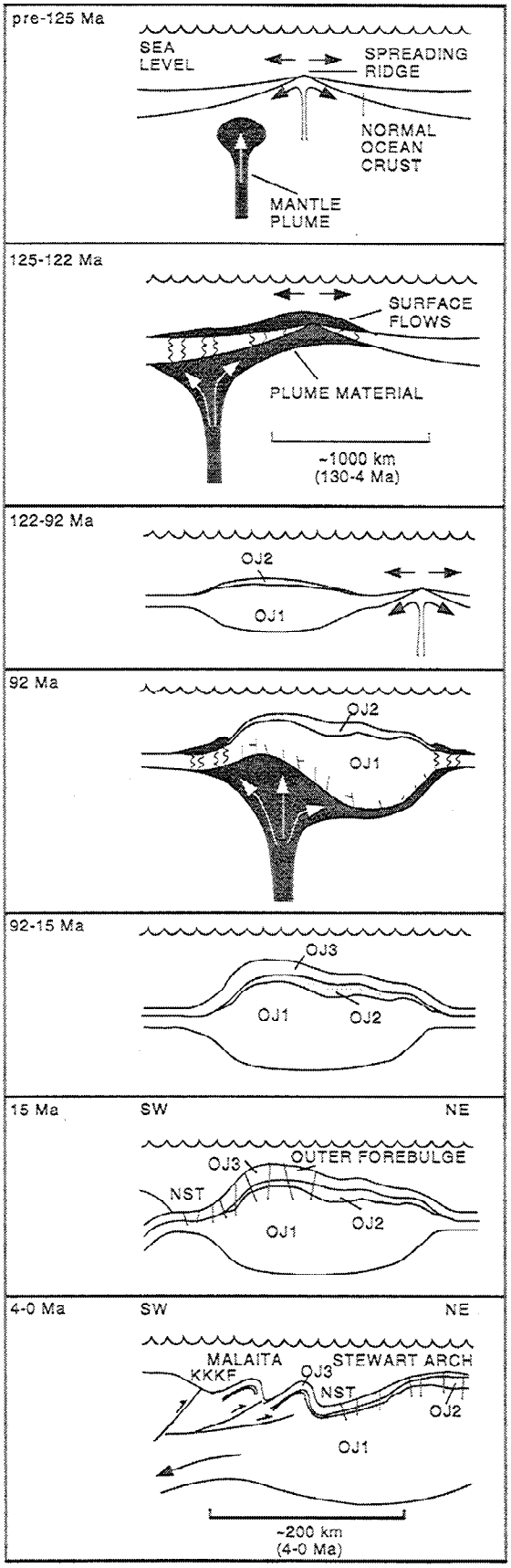

During deposition of OJ2, northward drift of the Pacific plate carried the southwest OJP well north of the Louisville hot spot (Figure 14b). However, OJP's northern margin had begun to pass over the Easter hot spot by 92 Ma. Radiometric dates of 92 Ma have been determined from both the northern OJP (ODP Site 803) and Santa Isabel in the MAP (Figure 1a). We propose that folding, faulting, uplift, and erosion of OJ2 is related to the Easter hot spot underplating existing 122 Ma old OJP lithosphere and/or underplating related to a second plume head linked to OJP's passage over the Louisville hot spot [*Bercovici and Mahoney*, 1994]. In either case, 92 Ma basalts at opposite ends of the OJP may reflect ponding of plume material beneath the 122 Ma old OJP and leakage upward at its edges (Figure 13).

The thicker northeast section of OJ2 was deposited on a paleobathymetric high created by the first mantle plume event at 125-122 Ma. Paleobathymetry also controlled the thinning of OJ2 to the southwest towards the North Solomon Trench as we infer the thinning to represent a flank of the original plateau. Thinning of the plateau sediment column with increasing water depth has been previously reported by *Mosher et al.* [1993] and is also observable on recent seismic data collected by M. F. Coffin et al. (personal communcation, 1998). The second mantle plume event uplifted, eroded, and gently folded OJ2 along the flank of the original plateau creating a new bathymetric high (Figure 13). A complementary mechanism for submarine erosion of OJ2 is the release of carbon dioxide associated with volcanism from a mantle plume that could have altered ocean chemistry, raised the CCD, and caused a dissolution event across OJP [*Coffin and Eldholm*, 1994]. After a brief depositional hiatus, uplift from the second mantle plume and/or lowering of the CCD allowed for deposition of pelagic carbonate. The reestablished carbonate sedimentation marked the beginning of OJ3.

Figure 13. (opposite) Schematic diagram illustrating tectonic history of the OJP. For pre-125 Ma late Jurassic to early Cretaceous oceanic crust forms at a spreading ridge. From 125 to 122 Ma initial mantle plume surfaces and erupts OJ1 in a near-ridge setting. From 122 to 92 Ma OJ2, marine mudstone (Kwaraae formation), is deposited in a moderately low-energy pelagic environment near a fluctuating CCD. At 92 Ma second mantle plume underplates and uplifts OJP resulting in gentle folds and submarine erosion of OJ2. Volcanism leaks upward at the edges of OJP. Subsequent differential subsidence may have resulted in later faulting of OJ2 and upper plateau crust. From 92 to 15 Ma late Cretaceous and Cenozoic pelagic megasequence OJ3 is deposited in a low-energy environment above the CCD. Around 15 Ma normal faulting affects the upper crust and sedimentary megasequences. Faulting appears related to flexure of OJP as it approaches the North Solomon Trench. From 4 to 0 Ma. after subduction reversed polarity in the late Miocene, impeded subduction along the San Cristobal trench results in middle Pliocene overthrusting of the Solomon Islands arc and accretion of OJP sediment and upper igneous crust. Subduction of OJP and crustal loading results in an outer forebulge with associated subparallel normal faults. Uppermost crust of OJP is currently being accreted while mid- and lower crust is subducted.

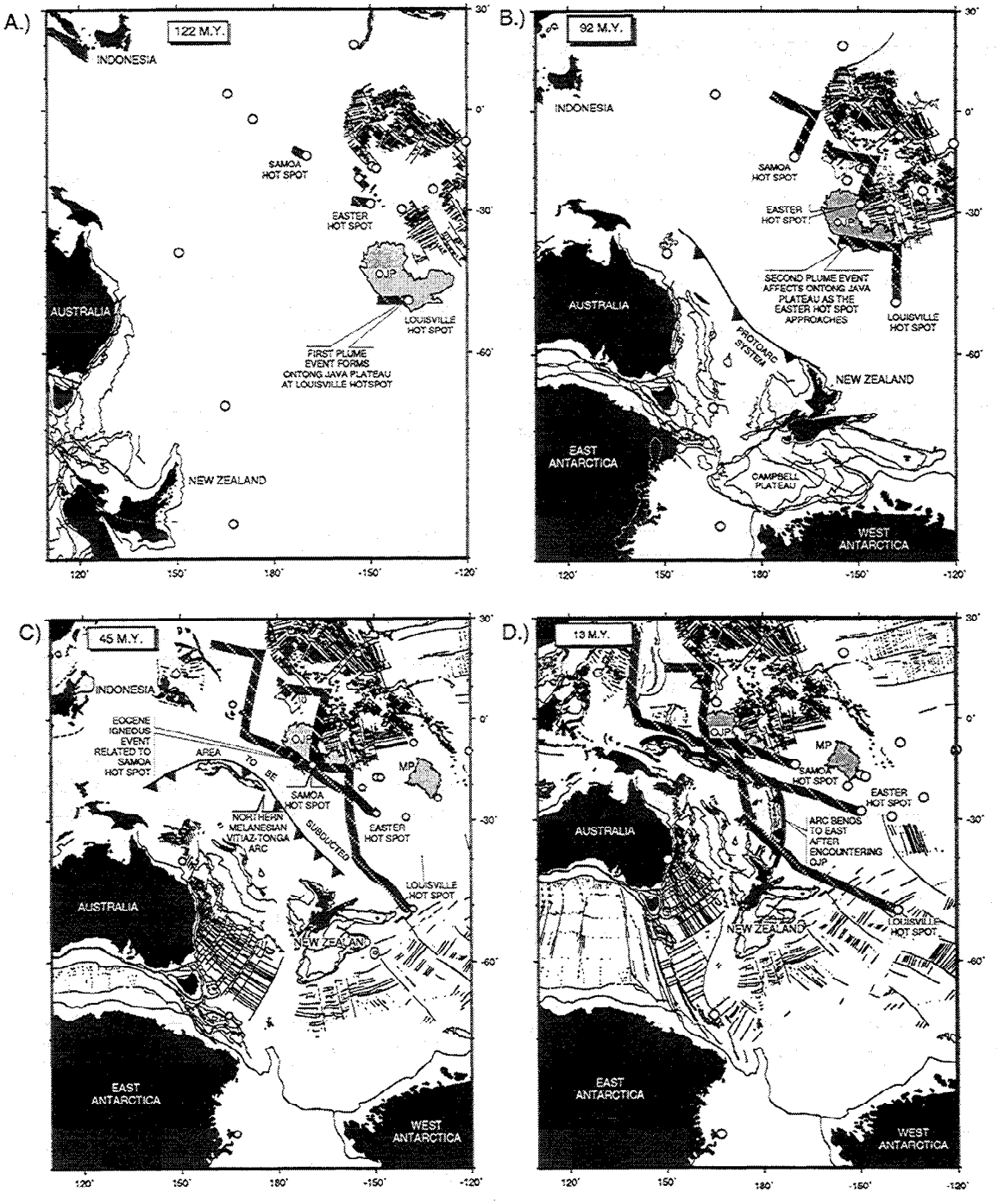

Figure 14. Plate reconstructions of the western Pacific at (a) 122, (b) 92, (c) 45, and (d) 13 Ma. These reconstructions are based on hierarchical closure of large and smaller plate pairs, including Pacific-Antarctica [*Cande et al.*, 1995]; Australia-Antarctica [*Royer et al.*, 1988; *Royer and Chang*, 1991; *Yan and Kroenke*, 1993]; opening of the Coral Sea and Woodlark basins [*Lee and Lawver*, 1995]; and opening of the North Fiji Basin [*Malahoff et al.*, 1982; *Auzende et al.*, 1988]. Reconstructions are simplified to show relationships among the Louisville, Easter, and Samoa hot spot tracks, OJP, and a continuous northern Melanesian-Vitiaz-Tonga island arc. More detailed regional reconstructions show positions and effects of other hot spots and multiple arc systems [*Yan and Kroenke*, 1993]

4.4. Period from 92 to 15 Ma: Deposition of Marine Pelagic Sediment (OJ3)

Late Cretaceous/Cenozoic sediment on OJP consists of a relatively uniform sheet of marine pelagic carbonate which has been well characterized by ODP drilling on the northern OJP (Figures 3e and 3f), by on land mapping in the MAP (Figure 3a), and by seismic reflection studies on the OJP [e.g., *Kroenke*, 1972; *Berger et al.*, 1991; *Mosher et al.*, 1993]. Plate reconstructions show that the OJP generally moved northwestward relative to the Samoa, Louisville, and Easter hot spots during this interval (Figures 14c and d). Small alnoite intrusions and alkali basalt flows within the pelagic carbonate section of Malaita have been dated at 34 Ma [*Davis*, 1977] and may relate to the southwestern OJP passing over the Samoa hot spot (Figure 14c).

The thickness of pelagic marine sediments capping the OJP is inversely proportional to water depth across most of the plateau, including its transitions into the adjoining Nauru and Lyra Basins, where sediment thins up to 65% between 2000 and 4000 m water depth [*Mosher et al.*, 1993] (Figure 1b). A major exception to this inverse relationship is on the southern margin of the plateau along line 1, where OJ3 thickens with water depth into the North Solomon Trench (Figure 1b).

From these observations we conclude that the accreted section of OJP forming the MAP from the southeastern end of Santa Isabel to Ulawa was previously bathymetrically higher than the section of OJP currently on the crest of the Stewart Arch. As stated previously, this structural high was created by uplift of OJ2 during the Cenomanian via magmatic underplating. The high maintained its position relative to the surrounding areas of the plateau until subduction during the latest Miocene and Pliocene (Figure 13).

4.5. Period Around 15 Ma: Normal Faulting

Two later periods of faulting are inferred from structural and stratigraphic relationships in OJ3 and are related to early entry of OJP into the North Solomon Trench (Figure 13). The first period, the cause for which is unclear, appears to postdate R34, which is tentatively dated as middle-late Miocene. Along line 1, multiple faults terminate at R34 (Figure 9). Northeast thickening below R34 near CMP 925 indicates limited syndepositional faulting. Plate reconstructions [*Mann et al.*, 1993] (Figure 14d) position the current leading edge of the OJP over 400 km northeast of the North Solomon subduction zone during this time.

4.6. Period from 4.6 to 4.0 Ma: Faulting and Flexure of OJP From Collision With Solomon Islands Arc

The most recent episode of faulting is most likely related to plate flexure of the OJP along the Stewart Arch associated with subduction [*Watts and Talwani*, 1974; *Cooper and Taylor*, 1985; *Levitt and Sandwell*, 1995] (Figure 13). As Plio-Pleistocene subduction and accretion at the North Solomon Trench depressed the current leading edge of the OJP, they concurrently caused uplift and flexure of the subducting OJP (Figure 13). Displacement along the faults increases seaward from the North Solomon Trench. An increase of 100 ms in post-R34 sediment thickness between blocks E and F (Figure 2) may also indicate some strike-slip motion. Based on the southwest convergence vector between the Pacific plate and the Solomon Islands (Figure 1), we postulate that motion is sinistral.

5. Conclusions

The first multichannel seismic data collected across the southernmost OJP adjacent to the North Solomon Trench image a more diverse sedimentary section than previously recognized. We divide the uppermost crust of the southern OJP into three megasequences: early Cretaceous basaltic basement (OJ1), Cretaceous deep-water mudstone and possibly carbonate (OJ2), and late Cretaceous through Cenozoic pelagic carbonate (OJ3). We show that previously interpreted intrabasement reflections are actually sedimentary in origin and correlate a previously interpreted igneous basement horizon with a late Cretaceous unconformity between two sedimentary megasequences.

Upper crustal velocities derived from multichannel seismic data are ~1 km/s lower than refraction values in the upper OJP crust. We are unable to correlate deep intrabasement reflections in OJ1 with stratigraphy or structure on nearby Malaita in the Solomon Islands. The most prominent of these reflections originate from impedance contrasts between basalt flows and sediment interbeds. Less prominent intrabasement reflections may be caused by either peg-leg multiples originating in the overlying megasequences or converted modes at the sediment/basalt transition. Eruption of the basalts forming OJ1 is correlated to the 122 Ma mantle plume event (Figure 13).

We correlate OJ2 with the Kwaraae Mudstone Formation on Malaita. OJ2, which consists almost entirely of claystone/ mudstone near the North Solomon Trench and on Malaita, changes composition laterally to the northeast as the layer thickens to >1000 m. Reflection configurations within OJ2 indicate deposition within a moderately low-energy environment near the CCD. Sediment thickness and erosion of OJ2 indicates uplift with shallow current erosion and/or dissolution related to a 92 Ma mantle plume event (Figure 13).

The Cenomanian to Recent depositional history of the OJ3 pelagic section capping the plateau differs from that of underlying OJ2. Conformable reflections indicate a lower-energy deep-sea environment above the CCD. The entire section of OJ3 can be correlated to Malaita and tentatively to DSDP Site 288. Multiple episodes of faulting affect OJ3: one occurred before deposition of the R34 horizon in the middle-late Miocene and another is related to mid-Pliocene plateau flexure caused by subduction (Figure 13).

We postulate the magmatic, tectonic, and sedimentary history of the southern OJP as follows. After the initial mantle plume event at 122 Ma, which created OJ1, OJ2 was deposited in a marine environment near the CCD with the area near the central part of line 1 being a bathymetric high characterized by higher sedimentation rates (Figure 14a). At 92 Ma the southern OJP was uplifted by underplating from a second mantle plume event resulting in submarine erosion/dissolution of OJ2 (Figure 14b). Differential uplift and subsidence resulted in faulting of OJ1 and OJ2. The southwestern OJP remained a structural high relative to surrounding parts of the plateau from late Cretaceous through Pliocene and accumulated a thicker OJ3 section

through higher sedimentation rates (Figure 14c). During the middle Miocene, OJ3 was faulted. Forebulge flexure likely did not cause this faulting because of the significant reconstructed distance between OJP and the North Solomon Trench at this time (Figure 14d). A second episode of OJ3 faulting is ongoing as the OJP flexes into the North Solomon Trench.

Acknowledgments. This paper is based on one chapter of a master's thesis by Phinney supported by UTIG during 1995-6 (Phinney, 1997). Phinney thanks P. Stoffa and the UTIG student cruise fund for the opportunity to participate in the EW95-11 cruise and work on these data. We thank K. Suyehiro, A. Taira, and E. Araki of the Ocean Research Institute of the University of Tokyo and M. Shinohara and S. Miura of Chiba University for discussions and their assistance during the collection of these data during EW95-11. We thank M.Petterson of the British Geological Survey for discussions and providing us with his unpublished report on the geology of Malaita, Santa Isabel and surrounding islands. We also thank L.Gahagan and L. Lawver and the UTIG PLATES project for the reconstructions of the OJP and associated hot spots shown in Figure 14. We thank the captain and crew of R/V *Maurice Ewing*, the Lamont-Doherty technical team for excellent support at sea, and S. Saustrup and D. Kakas of UTIG for their assistance in seismic data processing. We are grateful to Paul Wessel and Walter Smith for GMT software and databases. This work was supported by NSF/OCE-9301608 to Mann, Coffin, and Shipley. UTIG contribution 1409.

References

Auzende, J. M., Y. Lafoy, and B. Marsset, Recent geodynamic evolution of the North Fiji Basin (southwest Pacific), *Geology, 16*, 925-929, 1988.

Bercovici, D., and J. Mahoney, Double flood basalts and plume head separation at the 660-km discontinuity, *Science, 266*, 1367-1369, 1994.

Berger, W.H., and L.A. Mayer, Deep-sea carbonates: Acoustic reflections and lysocline fluctuations, *Geology, 6*, 11-15, 1978.

Berger, W.H., L.W. Kroenke, L.A. Mayer, and Shipboard Scientific Party, Ontong Java Plateau, Leg 130: Synopsis of major drilling results, *Proc. Ocean Drill. Program, Initial Rep., 130*, 497-537, 1991.

Cande, S.C., J.L. LaBrecque, R.L. Larson, W.C. Pitman III, X. Glovochenko, and W.F. Haxby, Magnetic lineations of the world's ocean basins, *AAPG Map Ser.*, 13, 1989.

Cande, S. C., Raymond, C. A., Stock, J., and Haxby, W. F., Geophysics of the Pitman fracture zone and Pacific-Antarctic plate motions during the Cenozoic, *Science, 270*, 947-953, 1995.

Coffin, M.F., and O. Eldholm, Large igneous provinces: Crustal structure, dimensions, and external consequences, *Rev. Geophys., 32*, 1-36, 1994.

Coffin, M.F., and L.M. Gahagan, Ontong Java and Kerguelan Plateaux: Cretaceous Icelands?, *J. Geol. Soc. London, 152*, 1047-1052, 1995.

Cooper, P., and B. Taylor, Polarity reversal in the Solomon Island arc, *Nature, 314*, 428-430, 1985.

Davis, G.L., The ages and uranium contents of zircons from kimberlites and associated rocks. paper presented at *2nd International Kimberlite Conference*, AGU, Santa Fe, N.M., 1977.

DeMets, C., R.G. Gordon, D.F. Argus, and S. Stein, Effect of recent revisions to the geomagnetic reversal time scale on estimates of current plate motions, *Geophys. Res. Lett., 21*, 2191-2194, 1994.

Duncan, R.A., and M.A. Richards, Hotspots, mantle plumes, flood basalts, and true polar wander, *Rev. Geophys., 29*, 31-50, 1991.

Furumoto, A.S., J.P. Webb, M.E. Odegard, and D.M. Hussong, Seismic studies on the Ontong Java Plateau, 1970, *Tectonophysics, 34*, 71-90, 1976.

Gladczenko, T., M.F. Coffin, and O. Eldholm, Crustal structure of the Ontong Java Plateau: modeling of new gravity and existing seismic data, *J. Geophys. Res., 102*, 22,711-22,729, 1997.

Hagen, R.A., L.A. Mayer, D.C. Mosher, L.W. Kroenke, T.H. Shipley, and E.L. Winterer, Basement structure of the northern Ontong Java Plateau, *Proc. Ocean Drill. Program, Sci. Results, 130*, 23-31, 1993.

Hughes, G.W., and C.C. Turner, *Geology of southern Malaita, Bull. 2*, Solomon Islands Geol. Surv., Honiara, Solomon Islands, 80 pp., 1976.

Hughes, G.W., and C.C. Turner, Upraised Pacific Ocean floor, southern Malaita, Solomon Islands, *Geol. Soc. Am. Bull., 88*, 412-424, 1977.

Hussong, D., L. Wipperman, and L. Kroenke, The crustal structure of the Ontong Java and Manihiki oceanic plateaus, *J. Geophys. Res., 84*, 6003-6010, 1979.

Kroenke, L., Geology of the Ontong Java Plateau, Ph.D. dissertation, 119 pp., *Univ. of Hawaii*, 119 p., Honolulu, 1972.

Kroenke, L.W., Interpretation of a multi-channel seismic-reflection profile northeast of the Solomon Islands from the southern flank of the Ontong Java Plateau across the Malaita Anticlinorium to the Solomon Islands arc, in *Geology and Offshore Resources of Pacific Island Arcs—Solomon Islands and Bougainville, Papua New Guinea Regions, Earth Sci. Ser.*, edited by J.G. Vedder and T.R. Bruns, Circum-Pac. Counc. for Energy and Miner. Resour., vol. 12, Houston, Tex., 1989.

Larson, R.L., Superplume and ridge interactions between Ontong Java and Manihiki Plateaus and the Nova-Canton Trough, *Geology, 25*, 779-782, 1997.

Lee, T. Y., and L. A. Lawver, Cenozoic plate reconstruction of southeast Asia, *Tectonophysics, 251*, 85-138, 1995.

Levitt, D.A., and D.T. Sandwell, Lithospheric bending at subduction zones based on depth soundings and satellite gravity, *J. Geophys. Res., 100*, 379-400, 1995.

Malahoff, A. R. H. Feden, and H. S. Fleming, Magnetic anomalies and tectonic fabric of marginal basins north of New Zealand, *J. Geophys. Res., 87*, 4109-4125, 1982.

Mann, P., L. Gahagan, and T.Y. Lee, Quantitative tectonic reconstruction of the diachronous collision of the Ontong Java Plateau along the 3000 km length of the northern Melanesian-Solomon—New Ireland convergent margin, *Eos Trans. AGU, 74*(43), Fall Meet. Suppl., 545, 1993.

Mann, P., M. Coffin, T. Shipley, S. Cowley, E. Phinney, A. Teagan, K. Suyehiro, N. Takahashi, E. Araki, M. Shinohara, and S. Miura, Researchers investigate fate of oceanic plateaus at subduction zones. *Eos Trans. AGU*, 77(30), 282-283, 1996.

Miura, S., M. Shinohara, N. Takahashi, E. Araki, A. Taira, K. Suyehiro, M. Coffin, T. Shipley, and P. Mann, OBS crustal structure of Ontong Java Plateau converging into Solomon Islands Arc, *Eos Trans. AGU, 77*(46), Fall Meet. Suppl., F713, 1996.

Mosher, D.C., L.A. Mayer, T.H. Shipley, E.L. Winterer, R.A. Hagen, J.C. Marsters, F. Bassinot, R.H. Wilkens, and M. Lyle, Seismic stratigraphy of the Ontong Java Plateau, *Proc. Ocean Drill. Program, Sci. Results, 130*, 33-49, 1993.

Nakanishi, M. and E.L. Winterer, Tectonic events of the Pacific Plate related to formation of Ontong Java Plateau, *Eos Trans. AGU , 77*(46), *Fall Meeting Suppl.*, F713, 1996.

Nakanishi, M., K. Tamaki, and K. Kobayashi, Magnetic anomaly lineations from late Jurassic to Early Cretaceous in the west-central Pacific Ocean, *Geophys. J. Int., 109*, 701-719, 1992.

Neal, C. R., J. J. Mahoney, L. W. Kroenke, R. A. Duncan, and M. G. Petterson, The Ontong Java Plateau, in *Large Igneous Provinces, Geophys. Monogr. Ser.*, vol. 100 edited by J. Mahoney and M. Coffin, AGU, Washington, D.C., pp. 183-216, 1997.

Petterson, M.G., *The Geology of North and Central Malaita, Solomon Islands*, Geol. Mem. 1/95, 219 pp., Water and Miner. Resour. Div., Minist. of Energy, Water and Miner. Resour., Honiara, Solomon Islands, 1995.

Petterson, M.G., C.R. Neal, J.J. Mahoney, L.W. Kroenke, A.D. Saunders, T.L. Babbs, R.A. Duncan, D. Tolia, and B. McGrail, Structure and deformation of north and central Malaita, Solomon Islands: Tectonic implications for the Ontong Java Plateau-Solomon arc collision, and for the fate of oceanic plateaus, *Tectonophysics, 283*, 1-33, 1997.

Phinney, E. J., Sequence stratigraphy, structure, and tectonics of the southern Ontong Java Plateau and Malaita accretionary prism, M.A. thesis, 128 pp., *Univ. of Tex. at Austin*, 1997.

Royer, J. Y., and T. Chang, Evidence for relative motions between the Indian and Australian plates during the last 20 Myr from plate tectonic reconstructions: Implications for the deformation of the Indo-Australian plate, *J. Geophys. Res., 96*, 11, 779-11,802, 1991.

Royer, J. Y., P. Patriat, H. Bergh, and C. Scotese, Evolution of the Southwest Indian Ridge from the late Cretaceous (anomaly 34) to the middle Eocene (anomaly 20), *Tectonophysics, 155*, 235-260, 1988.

Sandwell, D.T., and W.H.F. Smith, Marine gravity anomaly from Geosat and ERS-1 satellite altimetry, *J. Geophys. Res., 102*, 10,039-10,054, 1997.

Schlanger, S.O., and R.G. Douglas, The pelagic ooze-chalk-limestone transition and its implications for marine stratigraphy, *Spec. Publ. Int. Assoc. Sedimentol., 1*, 117-148, 1974.

Shipboard Scientific Party, Site 288, *Initial Rep. Deep Sea Drill. Proj., 30*, 175-230, 1975a.

Shipboard Scientific Party, Site 289, *Initial Rep. Deep Sea Drill. Proj. 30*, 231-398, 1975b.

Shipboard Scientific Party, Site 586, *Initial Rep. of the Deep Sea Drill. Proj., 89*, 213-281, 1986.

Shipboard Scientific Party, Site 803, *Proc. Ocean Drill. Program, Initial Rep., 130*, 101-175, 1991a.

Shipboard Scientific Party, Site 807, *Proc. Ocean Drill. Program, Initial Rep., 130*, 369-498, 1991b.

Shipley, T.H., L.J. Abrams, Y. Lancelot, and R.L. Larson, Late Jurassic-Early Cretaceous oceanic crust and Early Cretaceous volcanic sequences of the Nauru Basin, western Pacific, in *The Mesozoic Pacific: Geology, Tectonics, and Volcanism*, edited by M. Pringle et al., pp. 103-119, *Geophys. Monogr. Ser.*, vol. 77, AGU, Washington, D.C., 1993.

Tejada, M.L.G., J.J. Mahoney, R.A. Duncan, and M.P. Hawkins, Age and geochemistry of basement and alkalic rocks of Malaita and Santa Isabel, southern margin of the Ontong Java Plateau, *J. of Petrol., 37*(2), 361-394, 1996.

Watts, A.B., and M. Talwani, Gravity anomalies seaward of deep-sea trenches and their tectonic implications, *Geophys. J. R. Astron. Soc., 36*, 57-90, 1974.

Winterer, E.L., et al., Site 64 report, *Initial Rep. Deep Sea Drill. Proj., 7*, 473-606, 1971.

Winterer, E.L. and M. Nakanishi, Evidence for a plume augmented, abandoned spreading center on Ontong Java Plateau, *Eos Trans. AGU, 76(46)*, AGU Fall Meet. Suppl., F617, 1995.

Yan, C.Y., and L.W. Kroenke, A plate tectonic reconstruction of the southwest Pacific, 0-100 Ma, *Proc. Ocean Drill. Program, Sci. Results, 130*, 697-709, 1993.

M.F. Coffin, P. Mann, and T. H. Shipley, Institute for Geophysics, University of Texas at Austin, 4412 Spicewood Springs Road, Bldg. 600, Austin, TX 78759-8500. (paulm@utig.ig.utexas.edu)

E. J. Phinney, BP/Amoco, 501 Westlake Park Blvd., Houston, TX 77079. (phinneej@bp.com)

(Received April 8, 1998; revised December 15, 1998; accepted May 3, 1999.)